

Are your **MRI contrast agents** cost-effective?

Learn more about generic **Gadolinium-Based Contrast Agents**.



**FRESENIUS  
KABI**

caring for life

**AJNR**

**Multidetector Row CT Angiography in  
Spontaneous Lobar Intracerebral  
Hemorrhage: A Prospective Comparison with  
Conventional Angiography**

D.Y. Yoon, S.K. Chang, C.S. Choi, W.-K. Kim and J.-H.  
Lee

This information is current as  
of April 19, 2024.

*AJNR Am J Neuroradiol* 2009, 30 (5) 962-967

doi: <https://doi.org/10.3174/ajnr.A1471>

<http://www.ajnr.org/content/30/5/962>

**ORIGINAL  
RESEARCH**

D.Y. Yoon  
S.K. Chang  
C.S. Choi  
W.-K. Kim  
J.-H. Lee

# Multidetector Row CT Angiography in Spontaneous Lobar Intracerebral Hemorrhage: A Prospective Comparison with Conventional Angiography

**BACKGROUND AND PURPOSE:** The aim of our study was to assess the accuracy of multidetector row CT angiography (MDCTA) in the detection of the underlying vascular abnormalities causing spontaneous lobar intracerebral hemorrhage (ICH) compared with conventional digital subtraction angiography (DSA).

**MATERIALS AND METHODS:** Seventy-eight patients who underwent MDCTA with use of a 16-detector row scanner and DSA were prospectively included in this study. Each study was assessed by 2 independent blinded neuroradiologists; decisions were made in consensus. Findings on CT angiograms, including the original axial data, multiplanar reformations, and volume-rendered images with and without automated bone segmentation, were used to identify the underlying causes of ICH.

**RESULTS:** Twenty-two of the 78 patients (28.2%) exhibited angiographic abnormalities, including aneurysms of the proximal arteries ( $n = 9$ ), arteriovenous malformations ( $n = 7$ ), Moyamoya disease ( $n = 4$ ), and aneurysms of the distal arteries ( $n = 2$ ). MDCTA detected the underlying vascular abnormalities in 21 patients except 1 case of small arteriovenous malformation. Overall sensitivity, specificity, positive predictive value, negative predictive value, and accuracy of MDCTA for detection of underlying vascular abnormalities were 95.5%, 100%, 100%, 98.2%, and 98.7%, respectively.

**CONCLUSIONS:** MDCTA is a highly accurate imaging technique in the diagnosis of underlying vascular abnormalities in patients with spontaneous lobar ICH.

Lobar intracerebral hemorrhage (ICH) is defined as supratentorial hemispheric parenchymal bleeding located outside the deep nuclear structures and accounts for 20%–44% of all cases of ICH.<sup>1,2</sup> Hypertension is the most common cause of spontaneous ICH in the deep regions such as the basal ganglia, thalamus, pons, and cerebellum. However, lobar ICH is a separate group of supratentorial hemorrhage and the result of heterogeneous etiologies, including aneurysms, arteriovenous malformations (AVMs), amyloid angiopathy, cavernous angiomas, vasculitis, primary or metastatic tumors, Moyamoya diseases, cerebral venous thromboses, systemic hypertension, bleeding diatheses, and sympathomimetic drugs.<sup>1</sup> In patients with lobar ICH, therefore, a prompt diagnosis of underlying structural vascular abnormalities, such as aneurysms and AVMs, is critical for determining the appropriate treatment.<sup>3</sup>

Digital subtraction angiography (DSA) has been the gold standard diagnostic test in this setting. However, this procedure is invasive and not always available in critically ill patients. Furthermore, DSA reportedly has a 1% risk of a disabling neurologic deficit and a 0.1% risk of mortality.<sup>4</sup> When compared with DSA, CT angiography (CTA) is a noninvasive imaging technique, which has proved valuable for identifying cerebrovascular lesions. It can be easily performed immediately after the initial nonenhanced CT with a single bolus of intravenous contrast medium, thereby allowing rapid diagno-

sis and treatment planning in emergency conditions. The introduction of multidetector row CT (MDCT) has promoted the use of CTA for assessing the cerebrovascular system, offering a shorter acquisition time, increased volume coverage, and improved spatial resolution.<sup>5,6</sup>

To our knowledge, no study has examined the diagnosis of underlying causes of lobar ICH by using MDCT angiography (MDCTA). The purpose of our study was to compare prospectively the effectiveness of 16-channel MDCTA with that of conventional DSA in the detection of the underlying vascular abnormalities causing spontaneous lobar ICH.

## Materials and Methods

### Patient Population and Study Design

Between September 2004 and February 2008, 105 consecutive patients with spontaneous lobar ICH were referred to our institution. The patients were scheduled to undergo conventional DSA and were prospectively enrolled to undergo comparative MDCTA. Of them, 10 patients who did not undergo DSA due to rapid clinical deterioration were excluded from the study. Another 17 patients were also excluded from our study for the following reasons: 1) subarachnoid hemorrhage (SAH)-predominant cases ( $n = 8$ ), 2) known pre-existing cerebral vascular abnormalities ( $n = 6$ ), or 3) hemorrhage into a tumor diagnosed by CT or MR imaging ( $n = 3$ ). The final study group, therefore, consisted of 78 patients; this group included 44 men and 34 women (mean age,  $48.4 \pm 13.7$  years; range, 21–86 years).

Unenhanced CT revealed 23 frontal, 22 temporal, 16 parietal, 9 occipital, and 8 multiple lobar ICHs. Forty-four patients had pure lobar ICHs, 18 had coexistent SAH, 8 had associated intraventricular hemorrhage (IVH), 6 had both IVH and SAH, and 2 had subdural hemorrhage accompanying their lobar ICHs.

Received September 12, 2008; accepted after revision November 24.

From the Departments of Radiology (D.Y.Y., S.K.C., C.S.C.) and Neurology (W.-K.K., J.-H.L.), Hallym University College of Medicine, Seoul, Korea.

Please address correspondence to Dae Young Yoon, MD, Department of Radiology, Kangdong Seong-Sim Hospital, Hallym University College of Medicine, 445 Gil-dong Kangdong-Gu, Seoul, 134-701, Korea; e-mail: evee0914@chollian.net

DOI 10.3174/ajnr.A1471

**Table 1: Characteristics of patients and aneurysms**

Patient No.	Age (yr)/ Sex	Location	N/D Ratio		Orientation		Lobularity		Branches from Aneurysm		Severe Vasospasm*	
			DSA	MDCTA	DSA	MDCTA	MDCTA	DSA	DSA	MDCTA	DSA	MDCTA
1	48/F	AcomA	<1/3	Same	Anterior	Same	Multi-	Same	(-)	Same	Bilateral A1, A2; left M2	
2	40/F	MCAB	<1/3	1/3–2/3	Superior	Same	Single-	Same	(-)	Same	(-)	Same
3	56/M	MCAB	1/3–2/3	Same	Superior	Same	Multi-	Same	Neck	Same	(-)	Same
4	33/F	AcomA	>2/3	Same	Inferior	Same	Multi-	Same	(-)	Same	(-)	Same
5	39/F	AcomA	<1/3	Same	Superior	Same	Single-	Same	(-)	Same	(-)	Same
6	54/M	MCAB	<1/3	Same	Inferior	Same	Single-	Same	Neck	Same	(-)	Same
7	40/M	Distal ICA	>2/3	Same	Superior	Same	Multi-	Same	(-)	Same	(-)	Same
8	51/M	MCAB	1/3–2/3	Same	Lateral	Same	Single-	Same	Dome	Same	Right M2	
9	42/F	MCAB	>2/3	Same	Lateral	Same	Multi-	Same	Neck	Same	(-)	Same
10	46/M	Distal MCA	1/3–2/3	Same	Superior	Same	Single-	Same	(-)	Same	(-)	Same
11	44/M	Distal ACA	1/3–2/3	Same	Anterior	Same	Single-	Same	(-)	Same	(-)	Same

**Note:**—AcomA indicates anterior communicating artery; MCAB, MCA bifurcation; A1, first segment of the ACA; A2, second segment of the ACA; M2, second segment of the MCA; DSA, digital subtraction angiography; ICA, internal carotid artery; MCA, middle cerebral artery; ACA, anterior cerebral artery.  
\* Arterial spasm was categorized as severe when the vessel diameters were reduced by >50%.

**Table 2: Characteristics of patients and AVMs**

Patient No.	Age (yr)/ Sex	Location	Feeding Arteries		Nidus		Draining Veins	
			DSA	MDCTA	DSA	MDCTA	DSA	MDCTA
1	29/M	Frontal lobe	ACA	Same	Visible	Same	Cortical veins, SSS	
2	25/F	Frontal lobe	ACA	Not visible	Visible	Not visible	Deep veins, ICV	
3	44/F	Frontal lobe	MCA, ACA	Not visible	Visible	Same	Cortical veins, SSS	
4	30/F	Temporal lobe	MCA	Same	Visible	Same	Cortical veins, SSS	
5	35/F	Frontal lobe	ACA	Same	Visible	Same	Cortical veins, SSS	
6	31/M	Occipital lobe	PCA	Same	Visible	Same	Cortical veins, SS	
7	55/M	Parietal lobe	MCA	Not visible	Visible	Not visible	Cortical veins, SSS	

**Note:**—SSS indicates superior sagittal sinus; ICV, internal cerebral vein; SS, sigmoid sinus; AVM, arteriovenous malformation; PCA, posterior cerebral artery.

**Table 3: Characteristics of patients and Moyamoya disease**

Patient No.	Age (yr)/ Sex	Site of Occlusion		Collateral Vessels	
		DSA	MDCTA	DSA	MDCTA
1	28/F	Bilateral M1	Same	Basal	Not visible
2	31/F	Bilateral ICA	Same	Basal, leptomeningeal	
3	47/F	Bilateral ICA	Same	Basal, leptomeningeal, transdural	
4	38/F	Unilateral ICA	Same	Basal, leptomeningeal	

**Note:**—M1 indicates the first segment of the MCA.

**Table 4: Diagnostic performance of MDCTA for the detection of underlying vascular abnormalities causing spontaneous lobar intracerebral hemorrhage in 78 patients**

TP Cases	TN Cases	FP Cases	FN Cases	Sensitivity (%)	Specificity (%)	PPV (%)	NPV (%)	Accuracy (%)
21	56	0	1	95.5	100	100	98.2	98.7

**Note:**—TP indicates true-positive; TN, true-negative; FP, false-positive; FN, false-negative; PPV, positive predictive value; NPV, negative predictive value; MDCTA, multidetector row CT angiography.

The study protocol was approved by the institutional review board, and informed consent was obtained from all patients or their legal representatives.

**MDCTA and DSA**

All MDCTA scans were obtained by using a 16-detector row CT scanner (MX8000 Infinite Detector Technology; Philips, Haifa, Israel) with the following parameters: 1-mm section thickness; 0.5-second gantry rotation time; pitch of 0.35; 512 × 512 matrix; 20- to 22-cm FOV; 120 kV; and 200–280 mA. The scanning range was planned in a caudocranial direction from the level of the foramen magnum through the level of the top of skull, including the whole intracerebral vasculature (range, 120–140 mm). For optimal intraluminal contrast

enhancement, the delay time between the start of contrast material administration and the start of scanning was determined for each patient individually by using a bolus-tracking technique, as described in detail elsewhere.<sup>5,6</sup> A total of 100–120 mL of iohexol (Omnipaque 300; GE Healthcare, Princeton, NJ), a low-osmolar iodinated contrast material, was administered intravenously via an 18- or 20-gauge catheter positioned in an antecubital vein.

The volumetric data so obtained were transferred to a workstation with commercially available software (Rapidia 3D; Infinitt, Seoul, Korea) for further processing. Transverse sections were reconstructed with a section width of 0.5 mm. MDCTA images were processed from the obtained source images by using 3 different methods: 1) sagittal and coronal multiplanar reformations (MPRs), 2) volume-rendered

technique (VRT) algorithm, and 3) VRT after automatic segmentation of a precontrast scan dataset (ie, overlapping bony structures). All standardized reconstructions were completed by experienced technicians; image-processing time did not exceed 15 minutes.

Intra-arterial DSA was performed with femoral catheterization by the Seldinger technique with a DSA unit (Integris Allura; Philips Medical Systems, Best, the Netherlands) with an image-intensifier matrix of  $1024 \times 1024$  pixels. DSA was performed with bilateral selective internal carotid artery (ICA) injections and either unilateral or bilateral vertebral artery injections, as necessary. Anteroposterior, lateral, oblique, and, if necessary, additional views of each vessel were obtained by the injection of 6–9 mL of iodixanol (Visipaque 320, GE Healthcare) at a rate of 4–6 mL/s.

All patients in the series underwent MDCTA before DSA, with the longest interval between the 2 examinations being 36 hours (mean interval between examinations,  $16.1 \pm 9.0$  hours). Mean time from symptom onset to MDCTA was 9.8 hours (range, 6–28 hours).

### Interpretation and Analysis

All MDCTA and DSA images were independently evaluated by 2 neuroradiologists, who had 12 (D.Y.Y.) and 5 (S.K.C.) years of experience in CT vascular imaging and angiography. Interpretation disagreements were resolved by means of consensus review. The MDCTA and DSA images were presented in an anonymous random fashion. Both readers were blinded to the assessments of the other technique or of the other investigator. The MDCTA and DSA images were reviewed separately: DSA images were given in random order to the readers, 8 weeks after each reader completed the analysis of MDCTA images.

The standardized MPR and VRT images (as created by technicians) and axial CT images (source data) from MDCTA studies were available for both readers on the workstation. Both readers had the ability of rotating the standardized VRT images to obtain additional projections for better demonstration of the vascular lesion. The readers then could perform postprocessing reconstructions of the source image data again by using the various algorithms available at the workstation, if necessary.

Readers had to identify the underlying vascular abnormalities accounting for the hemorrhage on the images presented. The readers also had to describe morphologic features of the underlying vascular abnormalities (ie, lobularity; orientation of the dome; ratio of the neck to the dome [N/D ratio:  $<1/3$ ,  $1/3$ – $2/3$ , and  $>2/3$ ]; relationship to adjacent vessels; and presence of severe spasm [ $>50\%$  luminal narrowing] for aneurysms; size and shape of the nidus, feeding arteries, and draining veins for AVMs; and arterial occlusion and collateral vessels for Moyamoya disease). Moreover, the presence of coexisting vascular abnormalities, especially unruptured cerebral aneurysms, was also recorded.

The sensitivity, specificity, positive and negative predictive values, and accuracy of MDCTA for detection of underlying vascular lesions were calculated by using DSA as the standard of reference.

### Results

At DSA, a total of 22 patients (28.2%) had vascular abnormalities accounting for the hemorrhage: 9 had aneurysms of the proximal arteries, 7 had AVMs, 4 had Moyamoya disease, and 2 had aneurysms of the distal arteries. No secondary cause of ICH was identified by using DSA in the remaining 56 patients. In the non-angiographic-positive group, hypertension ( $n = 29$ ), coagulopathy ( $n = 11$ ), and amyloid angiopathy ( $n = 4$ )

were found as underlying causes of ICH; 14 patients had no clear cause of ICH.

Of the 11 ruptured aneurysms, 5 were located at the middle cerebral artery (MCA) bifurcation; 3 at the anterior communicating artery; 1, at the ICA bifurcation; 1, at the distal segment of the anterior cerebral artery (ACA); and 1, at the distal segment of the MCA. MDCTA correctly depicted all the 9 proximal and 2 distal aneurysms. According to MDCTA measurements (2 independent measurements were averaged for each aneurysm), the mean size of 11 aneurysms was  $4.9 \pm 2.2$  mm, and the smallest aneurysm was a 2.0-mm aneurysm in the distal MCA (Fig 1).

On DSA images, the N/D ratios were  $<1/3$  in 4,  $1/3$ – $2/3$  in 4, and  $>2/3$  in 3 aneurysms. In all but 1 aneurysm, the N/D ratio as assessed by MDCTA correlated well with the results of DSA; in 1 aneurysm, the N/D ratio was overestimated at MDCTA by 1 grade. MDCTA was also accurate in aneurysm characterization; orientation of the dome, lobularity, and relationship to adjacent vessels demonstrated by MDCTA corresponded well with the images obtained with DSA. In addition, MDCTA revealed severe vasospasm in 2 patients, which was confirmed by DSA (Table 1).

Of the 7 AVMs, 3 were in the ACA territory, 3 were in the MCA territory, and 1 was in the posterior cerebral artery (PCA) territory. The mean diameter of AVMs was  $11.8 \pm 5.0$  mm, and the smallest AVM was 4.0 mm in diameter. Only a 4.0-mm AVM without enlarged feeding or draining vessels could not be visualized by MDCTA. Except this case, all the AVMs detected by DSA were detected at the same locations by MDCTA (Fig 2). In all 6 patients with AVMs detected by MDCTA, MDCTA demonstrated the dilated draining veins leaving a nidus. In 1 patient with a 6-mm AVM, however, nidus and feeders were not demonstrated on MDCTA. In another patient who had a 10-mm AVM, MDCTA did not demonstrate feeders entering a nidus (Table 2).

Of 4 patients with Moyamoya disease, DSA demonstrated bilateral occlusion of the ICA ( $n = 2$ ), unilateral occlusion of the ICA ( $n = 1$ ), and bilateral occlusion of the proximal MCA ( $n = 1$ ) (Fig 3). Identical MDCTA findings were present in all patients. In 2 patients, however, MDCTA failed to depict fine collateral vessels in the basal brain (Table 3).

In summary, MDCTA detected the underlying vascular abnormalities in 21 cases except 1 case of a small AVM. There were no MDCTA false-positive results. Compared with DSA, the overall sensitivity, specificity, positive predictive value, negative predictive value, and accuracy of MDCTA for detection of underlying vascular abnormalities were 95.5%, 100%, 100%, 98.2%, and 98.7%, respectively (Table 4).

There were 2 patients with incidentally found vascular abnormalities: Each had an incidental noncausative aneurysm, which was apparent on both MDCTA and DSA. These aneurysms were located at the MCA bifurcation and the distal ICA, contralateral to the site of ICH, respectively.

### Discussion

It is often difficult to determine the underlying causes of ICH because vascular abnormalities such as AVM or aneurysm are not necessarily visualized in cross-sectional imaging studies. The site of hemorrhage, age of the patient, pre-existing hypertension, and hematoma extension to the ventricles or sub-

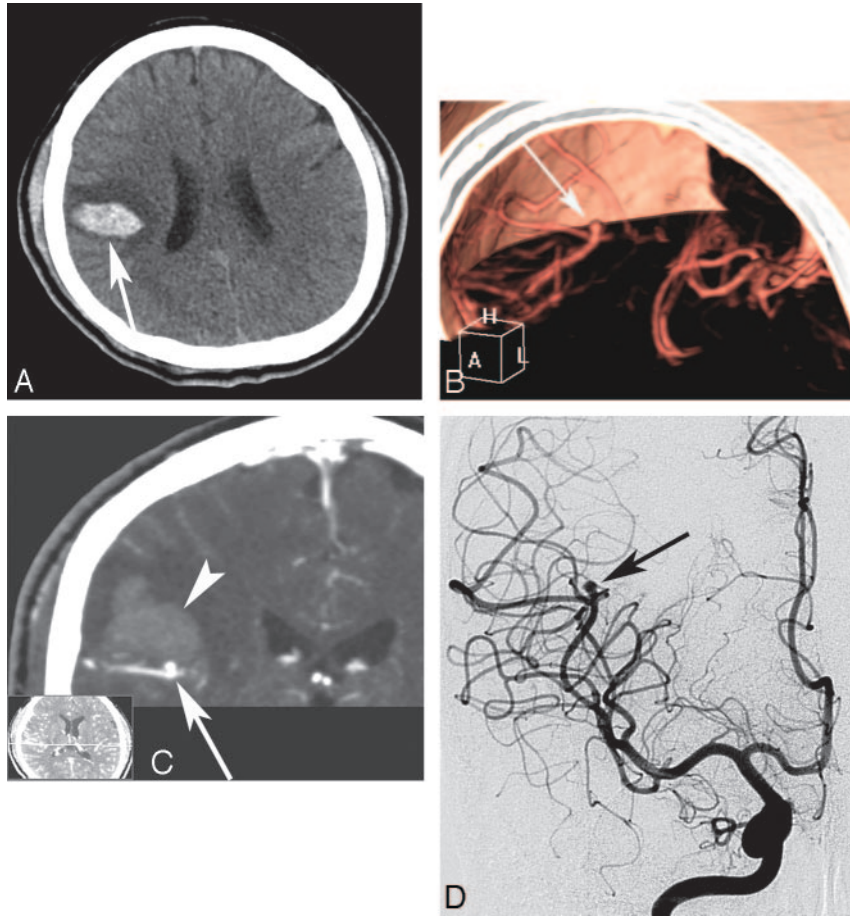


**Fig 1.** A 46-year-old man with an aneurysm of the distal MCA. *A*, Unenhanced CT scan demonstrates hemorrhage (*arrow*) in the right parietal lobe with mild surrounding edema. *B* and *C*, Left anterior oblique projection of the volume-rendered image (*B*) and the coronal multiplanar reformatted image (*C*) from MDCTA demonstrates a 2.5-mm saccular aneurysm (*arrow*) at the distal branch of the right MCA with an upward orientation of the sac. Note the relationship of the hematoma (*arrowheads*) to the aneurysm. *D*, DSA image of the right ICA, anteroposterior projection, shows the same aneurysm (*arrow*), which was confirmed at surgical exploration.



**Fig 2.** A 29-year-old man with an arteriovenous malformation. *A*, Unenhanced CT scan demonstrates hemorrhage (*arrow*) in the right frontal lobe. *B*, Volume-rendered MDCTA image, lateral projection, clearly demonstrates the abnormal collections of vessels in the right frontal lobe (*arrowhead*) and the enlarged draining cortical veins (*arrows*). *C*, Corresponding DSA image of the right ICA confirms these findings, demonstrating the nidus (*arrowhead*) and the early draining veins (*arrows*).

arachnoid space are important factors in determining the possibility of finding a vascular abnormality by DSA.<sup>2,7,8</sup> However, indications that DSA can find underlying potentially treatable vascular abnormalities still remain controversial.<sup>9,10</sup> The guidelines of the American Heart Association<sup>11</sup> recommend diagnostic DSA for all patients with no clear cause of hemorrhage who are candidates for surgery, particularly

young patients without hypertension whose condition is clinically stable.

CTA has been used to diagnose intracranial vascular diseases such as aneurysm,<sup>5</sup> arteriovenous malformation,<sup>12</sup> stenotic disease,<sup>13</sup> and vasospasm.<sup>6</sup> The advantages of CTA over DSA are that it is less invasive, is much quicker to perform, does not require sedation in most patients, and is

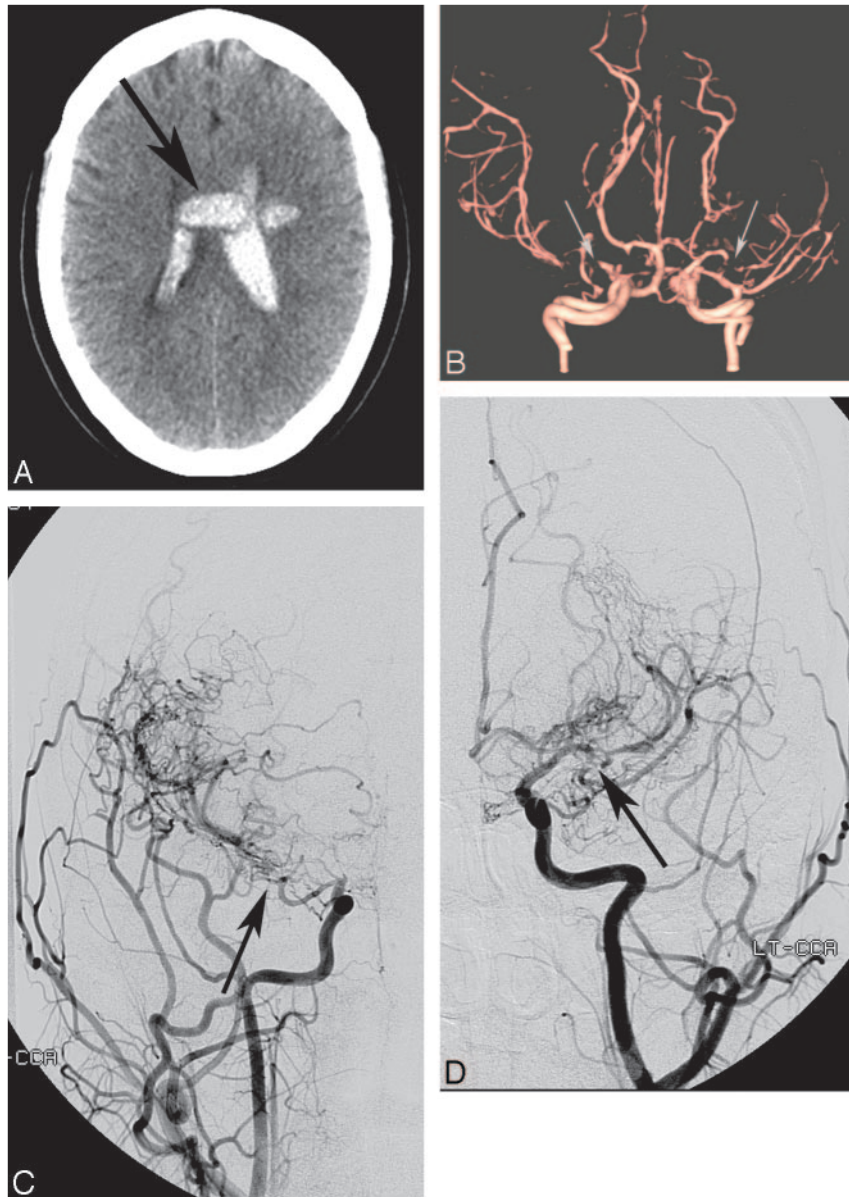


**Fig 3.** A 28-year-old woman with Moyamoya disease. *A*, Unenhanced CT scan demonstrates pericallosal hematoma (*arrow*) with extension of hemorrhage into the lateral ventricle. *B*, Volume-rendered MDCTA image with bone subtraction, anteroposterior projection, demonstrates symmetric occlusion of the bilateral proximal MCAs (*arrows*). MDCTA image fails to show collateral vessels. *C* and *D*, Corresponding DSA images of the right (*C*) and left (*D*) carotid arteries, anteroposterior projection, confirm occlusion of the bilateral proximal MCAs (*arrows*). In addition, reconstitution of the distal MCAs via fine collateral vessels is also noted.

suitable for emergency examinations of critically ill or unstable patients. CTA may, therefore, be useful in guiding the management of patients with acute spontaneous ICH, regarding the decision of whether to perform a further diagnostic study (DSA) versus surgery or follow-up.

With the introduction of MDCT scanners, there has been increased demand and use with regard to vascular applications.<sup>14</sup> Fundamental theoretic advantages of MDCT include substantially faster scanning speed, greater volumetric coverage, higher longitudinal spatial resolution, and more isotropic voxels than was possible with single-detector-row spiral CT scanners.<sup>15</sup> The major advantage of MDCTA is the ability to scan the whole brain within 1 acquisition, combined with a high spatial resolution, thus enabling the identification of vascular lesions not only of major cerebral arteries but also of distal intracerebral vessels. In this study, the scanning range

was planned to encompass the whole intracerebral vasculature from the level of the foramen magnum to the vertex, irrespective of the location of the ICH. The lack of comparable data in the literature is directly linked to the previous technologic limitations of CTA, which was based on single-detector-row spiral CT examinations of a limited region of interest.<sup>16</sup> MR angiography (MRA) is another noninvasive imaging method that can be used to identify underlying causes of ICH. MRA has the advantages of lack of exposure to ionizing radiation, no requirement for intravenous contrast medium, large volume coverage, and reasonably fast postprocessing. In addition, MR imaging can reveal amyloid angiopathy, cavernous angioma, and venous sinus thrombosis, which are less likely to be detected by using CT/CTA. MR/MRA, however, is not suitable in this patient group because of the relatively long examination time, difficulty in demonstrating vessels with low-flow condi-

tions (eg, the distal intracranial vessels), and limited access to the critically ill patients. To our knowledge, there are no data regarding the use of MRA in the detection of underlying vascular abnormalities in patients with spontaneous ICH.

To date, little has been reported on the role of CTA in spontaneous ICH. We found in the literature only 1 article<sup>16</sup> comparing DSA and CTA in the identification of causes of hemorrhage in patients with hyperacute ICH; however, the authors focused on contrast extravasation on CTA as a predictor of hematoma expansion. They analyzed 31 cases of primary ICH (they did not comment on the location of hemorrhage); angiography or surgery revealed vascular lesions in 7 (22.6%). In their study, by using a relatively small scanning range (from the skull base to the superior margin of the hematoma), single-detector-row CTA depicted the underlying vascular abnormality in all 7 patients.

To our knowledge, ours is the first study to examine the role of MDCTA in spontaneous lobar ICH. The results of our study showed that MDCTA had a diagnostic accuracy, which appeared equivalent to that of conventional DSA in the detection of underlying vascular abnormalities. The only false-negative case on MDCTA, a 4-mm AVM, was missed by both readers due to its small size, its linear configuration instead of a round shape, and its nonenlarged feeding and draining vessels. This AVM could not be clearly identified even on retrospective review of VRT and MPR images and the raw source images. However, MDCTA was inferior to DSA for the depiction of detailed morphologic characteristics of vascular lesions, such as N/D ratio of aneurysms, feeding arteries of AVMs, and fine collateral vessels in Moyamoya disease, which are important for planning treatment.

A limitation of this study relates to the small prevalence of underlying vascular abnormalities in our study group (28.2%), which is lower than that in previously published data, which ranged from 33.3% to 57.3%.<sup>2,8,9,17</sup> This relatively low prevalence may limit the calculated descriptive statistics for MDCTA versus conventional DSA. Another limitation of this study is that we did not address cost issues of MDCTA or DSA. Further investigations are warranted to compare MDCTA and DSA for evaluation of patients with spontaneous lobar ICH in terms of cost-effectiveness, because this analysis may also guide referring physicians to select MDCTA or DSA. Finally, we did not include patients with ICH in the deep regions such as the putamen, thalamus, cerebellum, and pons. In this group, only patients in whom MDCTA demonstrated vascular lesions underwent DSA at our institution.

In conclusion, MDCTA is a promising noninvasive method for the evaluation of underlying vascular abnormalities in patients with spontaneous lobar ICH. MDCTA is currently not sensitive enough to replace DSA; however, we believe that MDCTA may eliminate the need for conventional DSA angiography in selected cases.

## References

1. Ohtani R, Kazui S, Tomimoto H, et al. **Clinical and radiographic features of lobar cerebral hemorrhage: hypertensive versus non-hypertensive cases.** *Intern Med* 2003;42:576–80
2. Zhu XL, Chan MS, Poon WS. **Spontaneous intracranial hemorrhage: which patients need diagnostic cerebral angiography? A prospective study of 206 cases and review of the literature.** *Stroke* 1997;28:1406–09
3. Qureshi AI, Tuhim S, Broderick JP, et al. **Spontaneous intracerebral hemorrhage.** *N Engl J Med* 2001;344:1450–60
4. Hankey GJ, Warlow CP, Sellar RJ. **Cerebral angiographic risk in mild cerebrovascular disease.** *Stroke* 1990;21:209–22
5. Yoon DY, Lim KJ, Choi CS, et al. **Detection and characterization of intracranial aneurysms with 16-channel multidetector row CT angiography: a prospective comparison of volume-rendered images and digital subtraction angiography.** *AJNR Am J Neuroradiol* 2007;28:60–67
6. Yoon DY, Choi CS, Kim KH, et al. **Multidetector-row CT angiography of cerebral vasospasm after aneurysmal subarachnoid hemorrhage: comparison of volume-rendered images and digital subtraction angiography.** *AJNR Am J Neuroradiol* 2006;27:370–77
7. Laissy JP, Normand G, Monroc M, et al. **Spontaneous intracerebral hematomas from vascular causes: predictive value of CT compared with angiography.** *Neuroradiology* 1991;33:291–95
8. Loes DJ, Smoker WR, Biller J, et al. **Nontraumatic lobar intracerebral hemorrhage: CT/angiographic correlation.** *AJNR Am J Neuroradiol* 1987;8:1027–30
9. Toffol GJ, Biller J, Adams HP Jr, et al. **The predicted value of arteriography in nontraumatic intracerebral hemorrhage.** *Stroke* 1986;17:881–83
10. Halpin SF, Britton JA, Byrne JV, et al. **Prospective evaluation of cerebral angiography and computed tomography in cerebral haematoma.** *J Neurol Neurosurg Psychiatry* 1994;57:1180–86
11. Broderick JP, Adams HP Jr, Barsan W, et al. **Guidelines for the management of spontaneous intracerebral hemorrhage: a statement for healthcare professionals from a special writing group of the Stroke Council, American Heart Association.** *Stroke* 1999;30:905–15
12. Tanaka H, Numaguchi Y, Konno S, et al. **Initial experience with helical CT and 3D reconstruction in therapeutic planning of cerebral AVMs: comparison with 3D time-of-flight MRA and digital subtraction angiography.** *J Comput Assist Tomogr* 1997;21:811–17
13. Skutta B, Fürst G, Eilers J, et al. **Intracranial stenooclusive disease: double-detector helical CT angiography versus digital subtraction angiography.** *AJNR Am J Neuroradiol* 1999;20:791–99
14. Rubin GD, Shiau MC, Leung AN, et al. **Aorta and iliac arteries: single versus multiple detector-row helical CT angiography.** *Radiology* 2000;215:670–76
15. Kato Y, Nair S, Sano H, et al. **Multi-slice 3D-CTA: an improvement over single slice helical CTA for cerebral aneurysms.** *Acta Neurochir (Wien)* 2002;144:715–22
16. Murai Y, Takagi R, Ikeda Y, et al. **Three-dimensional computerized tomography angiography in patients with hyperacute intracerebral hemorrhage.** *J Neurosurg* 1999;91:424–31
17. Griffiths PD, Beveridge CJ, Gholkar A. **Angiography in non-traumatic brain haematoma: an analysis of 100 cases.** *Acta Radiol* 1997;38:797–802